http://dx.doi.org/10.15446/ing.investig.v41n2.83114

Multimetric Analysis of a Simulated Mixed Traffic of Motorcycles and Automobiles: Flow, Energy, CO_2 and Costs

Análisis Multimétrico de un Tráfico Mixto Simulado de Motocicletas y Automóviles: Flujo, Energía, CO_2 y Costos

Fábio Santana Magnani [1], Paulo D'Ávila Garcia Neto [2], Fernando Wesley Cavalcanti de Araújo [3], Alcides Luiz dos Anjos Hora [4], and Daniel Arraes de Alencar Valença [5]

ABSTRACT

The fleet of developing countries consists of motorcycles and cars. This heterogeneous traffic condition has its advantages and disadvantages, which results in conflicting points of view (*e.g.*, motorcyclists enjoying a higher mobility while car drivers resent their decreased speed). In this paper, we corroborated the notion that traffic evaluation depends on the chosen metric (*e.g.*, vehicle flow, fuel consumption, monthly costs) and the point of view (driver, rider, and policy makers). To this effect, we studied a mixed traffic condition, considering that the vehicle performance is affected by three scales: engine, vehicle, and traffic. We modeled the engine using empirical correlations of power and energy efficiency, the vehicle based on a balance of propulsive and resistive forces, and traffic with a cellular automata model. We simulated 189 traffic conditions and evaluated vehicle flow, average energy consumption, total CO_2 emission of the road, and monthly costs. We also discussed the results from the point of view of the driver, rider, and society. We concluded that the optimal condition depends both on the choice of metric and point of view, and that is not appropriate to use results from homogeneous traffic to analyze heterogeneous traffic conditions, even if both scenarios present the same total vehicle flow.

Keywords: car, motorcycle, traffic, CO_2, costs, cellular automata

RESUMEN

La flota de los países en vías de desarrollo está compuesta por motocicletas y automóviles. Esta condición heterogénea en el tráfico presenta ventajas y desventajas, lo que resulta en puntos de vista conflictivos (por ejemplo, los motociclistas que disfrutan de su mayor movilidad mientras que los conductores de automóviles se resienten con su velocidad disminuida). En este artículo corroboramos la idea de que la evaluación del tráfico depende de la métrica escogida (por ejemplo, flujo de vehículos, consumo de combustible, costos mensuales) y del punto de vista (conductor, motociclista y responsables de formular políticas). Para ello, estudiamos una condición de tráfico mixto, considerando que el rendimiento del vehículo se ve afectado por tres escalas: motor, vehículo y tráfico. Modelamos el motor usando correlaciones empíricas de potencia y eficiencia energética, la del vehículo a través de un equilibrio de fuerzas propulsoras y resistivas, y la del tráfico mediante un modelo de autómata celular. Simulamos 189 condiciones de tráfico y evaluamos el flujo de vehículos, el consumo de energía promedio, la emisión total de CO_2 de la vía y los costos mensuales. También discutimos los resultados desde el punto de vista del conductor, el motociclista y la sociedad. Llegamos a la conclusión de que la condición óptima depende tanto de la elección de la métrica como del punto de vista, además de que no es apropiado usar los resultados del tráfico homogéneo para analizar condiciones de tráfico heterogéneo, incluso si ambos escenarios presentan el mismo flujo total de vehículos.

Palabras clave: automóviles, motocicletas, tráfico, CO2, costos, autómata celular

Received: October 23rd, 2019
Accepted: January 7th, 2021

Introduction

Most of the fleets of developing countries such as Brazil, Colombia, Malaysia, Pakistan, Thailand, Philippines, and Nigeria consist of cars and motorcycles (WHO, 2015). In those countries, the use of motorcycles is motivated by the poor quality of transit, traffic congestion, and their advantageous cost of acquisition and operation, together with a higher average speed. On the other hand, motorcycle accidents are accountable for economic and social impacts (Koossalapeerom et al., 2019). The conflict between

[1]Mechanical Engineer, UFSC, Brazil. Dr. Mech. Eng., UFSC, Brazil. Affiliation: Associate Professor, UFPE, Brazil. E-mail: fabio.magnani@ufpe.br
[2]Mechatronic Engineer, UPE, Brazil. M.Sc. Mech. Eng., UFPE, Brazil. Affiliation: Assistant Professsor, IFPE, Brazil. E-mail: pdgneto@gmail.com
[3]Chemical Engineer, UFPE, Brazil. M.Sc. Mech. Eng., UFPE, Brazil. Affiliation: Ph.D. Candidate and Chemical Engineer, UFPE, Brazil. E-mail: fernando.wesley@ufpe.br
[4]Mechanical Engineer, UFPE, Brazil. M.Sc. Mech. Eng., UFPE, Brazil. Affiliation: Adjunct Lecturer, UFS, Brazil. E-mail: alcidesluiz@gmail.com
[5]Electronics Engineer, UFPE, Brazil. M.Sc. Mech. Eng., UFPE, Brazil. Affiliation: General Manager, Ameciclo, Brazil. E-mail: dvalenca@gmail.com

How to cite: Magnani, F. S., Garcia Neto, P. D., Araújo, F. W. C., Hora, A. L. A., and Valença D. A. A. (2021). Multimetric Analysis of a Simulated Mixed Traffic of Motorcycles and Automobiles: Flow, Energy, CO_2 and Costs. *Ingeniería e Investigación*, *41*(2). 10.15446/ing.investig.v41n2.83114

advantages and disadvantages addresses the relevance of the metric analyzed when evaluating traffic, which can be an individual one, such as travel time and direct costs; or a collective one, such as indirect costs with road infrastructure and accidents, flow of vehicles, fuel production, and CO_2 emissions (Tranter, 2012).

Traffic is a complex non-linear system affected by internal and external factors (Zegeye, De Schutter, Hellendoorn, Breunesse, and Hegyi, 2013) and it depends on instantaneous conditions such as vehicle density and the ratio of different types of vehicles. Homogeneous traffic flow models are unable to faithfully represent mixed traffic conditions, as it happens in developing countries (Agarwal, Zilske, Rao, and Nagel, 2015), in which motorcycles and passenger cars constitute the fleet and are accountable for significant emissions in major cities (Arun, Mahesh, Ramadurai, and Shiva Nagendra, 2017). Several papers claim that total vehicle flow varies for the same total density when mixed traffic occurs, increasing when there are motorcycles on the track, and decreasing when there are trucks, thus reflecting dynamic characteristics (Yang, Qiu, Yu, Sun, and Pu, 2015).

Furthermore, traffic cannot be evaluated only by its vehicle flow. Other metrics such as air pollution, CO_2 emission, direct costs, congestion, cost of changing the infrastructure, and accidents should also be taken into account (Gössling and Choi, 2015). Individual vehicle owners tend to purchase their vehicle based on flexibility and convenience. For motorcycles, low purchase and running costs are essential for the lower income population who acquire them (Koossalapeerom et al., 2019). There is also a growing concern about the global climate change, and CO_2 emissions from the transportation sector is a frequently addressed subject (Ehsani, Ahmadi, and Fadai, 2016).

This study contributes to the literature with the evaluation and discussion of different metrics such as flow, energy, CO_2, and costs, from the point of view of different stakeholders: drivers, motorcycle riders, and policy makers. Although the results from individual metrics are present in the literature, there is a lack of studies integrating the models and discussing the results. In order to evaluate those metrics, we applied a method that considers three scales: engine, vehicle, and traffic. We studied the engine using an empirical correlation of power and efficiency, the vehicle was studied modeling the propulsive and resistive forces, and the traffic with a cellular automata (CA) model, in which we simulated the traffic for 189 distinct density combinations of cars and motorcycles.

Methodology

The dynamic behavior and energy expenditure of vehicles depend on the engine, powertrain, chassis, traffic, driver/rider driving style, road/weather condition, and traffic laws. In this study, vehicle performance considers the engine, vehicle, and traffic. Other aspects are simplified, such as the driver/rider always trying to reach the maximum speed, the absence of traffic lights and intersections, and the road being a one-way straight line (Figure 1). This track model is based on the one proposed by Meng, Dai, Dong, and Zhang (2007), and it represents a single-track road for cars, with enough space for motorcycles to split and filter through them.

The engine is modeled by two empirical correlations. The cubic curve of the maximal power ($P_{\max,\text{eng}}$), Equation (1), is given by Ni and Henclewood (2008), and it is a function of engine speed (Ω). This model needs the following inputs: peak power, engine speed at peak power (Ω_p) and engine speed at peak torque (Ω_t).

$$P_{\max,\text{eng}}(\Omega) = \frac{P_{\max,\text{eng}}\,3\Omega\left(\Omega_p-\Omega_t\right)}{2\Omega_p^2} - \frac{P_{\max,\text{eng}}\,\Omega\left(\Omega-\Omega_t\right)^2}{2\Omega_p^2\left(\Omega_p-\Omega_t\right)} \tag{1}$$

The efficiency map in Equation (2) is described by Ben-Chaim, Shmerling, and Kuperman (2013), and it reports engine efficiency (η_{eng}) based on the engine's maximum efficiency ($\eta_{\text{eng},m}$), as well as considering factors related to engine speed (μ_r) and throttle usage (μ_a). A detailed explanation regarding the integration of both models can be found in Andrade, Araújo, Santos, and Magnani (2020).

$$\eta_{\text{eng}}(\Omega,\alpha) = n_{\text{eng},m}\,\mu_r\mu_a \tag{2}$$

Table 1 lists the parameters employed in this study to represent cars and motorcycles, reproducing characteristics of the usual Brazilian models. In average, Brazilian cars are lighter and less powerful than American and European cars.

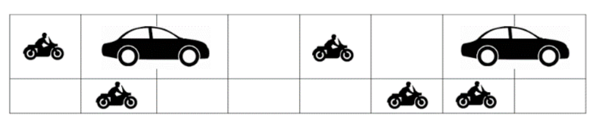

Figure 1. Based on Meng et al. (2007).
Source: Authors

Table 1. Engine and vehicle parameters employed in the simulation

Parameter	Car	Motorcycle
Peak power ($P_{\max,\text{eng}}$)	53,69 kW	8,53 kW
Engine speed at peak power (Ω_p)	6 250 rpm	8 250 rpm
Engine speed at peak torque (Ω_t)	4 500 rpm	6 000 rpm
Minimum engine speed	900 rpm	1 400 rpm
Max engine efficiency ($\eta_{\text{eng},m}$)	30%	
Rolling resistance coefficient (C_R)	0,02	
Vehicle + driver mass (m)	1 010 kg	175 kg
Transmission efficiency (η_{trans})	0,95	

Source: Authors

The dynamic behavior of the vehicle is based on the balance of propulsive and resistive forces (Equation 3) (Cossalter, 2006; Jazar, 2014). On the left-hand side of the equation is the inertia, where m is the total mass (vehicle + driver),

V is vehicle speed, and t is time. Tractive force considers $\alpha P_{\max,\text{eng}}$ as the actual power of the engine, and η_{trans} is the transmission efficiency. Throttle usage, α, is the ratio between the actual power and the maximum possible power at a specific engine speed. The braking force has β as the braking factor, μ as the friction coefficient between tire and road, and θ as the road grade. The aerodynamic drag force considers the constant k_A (*i.e.*, $1/2\rho AC_D$) with ρ as fluid density (air), A as the frontal area, C_D as the vehicle shape, and W is the wind speed. In the equation, rolling resistance, C_R, is also considered, as well as the gravitational resistance (mg), both related to road grade.

$$m\frac{dV}{dt} = \frac{\alpha P_{\max,\text{eng}}\,\eta_{\text{trans}}}{V} - \beta\mu\ \text{mgcos}\theta - k_A(V-W)^2 - C_R\ \text{mgcos}\theta - \text{mgsin}\theta \tag{3}$$

The finite difference method is used to solve the balance of forces in Equation (3). For every time step t, this Equation is employed to calculate factors α (throttling) and β (braking) to obtain the desired speed (restricted by the traffic condition, *i.e.*, the speed and position of nearby vehicles, as well as pilot preferences, who may always try to reach the maximum allowed speed as soon as it is physically possible). Thus, those calculated α and β values (limited to the range [0-1]) are reused in Equation (3) to determine the actual instantaneous speed V (in opposition to the original desired speed). As α and β are limited (modelling the limits of the acceleration and braking powers), the actual vehicle speed will not always be equal to the desired one. With the evolution of α (related to the throttle opening) during the vehicle movement, it is possible to calculate the vehicle energy expenditure during a time interval Δt using Equation (4):

$$e = \int_0^{\Delta t} \frac{\alpha P_{\max,\text{eng}}}{\eta_{\text{eng}}} dt \tag{4}$$

Modelling the vehicle (Equations 3 and 4) depends on the engine model and the desired speed, which must result from the traffic model. In this study, the employed traffic model is a cellular automata (CA) model based on Meng et al. (2007). This microscopic traffic model considers the individual movement and interactions of each vehicle in heterogeneous traffic conditions. The CA model is discrete for position and time, but, even with its simplicity, it is able to reproduce complex traffic phenomena, *e.g.* the start-stop waves that appear in congested traffic. The CA model is also known as the NaSch model, an abbreviation from the researchers that first employed the model: Nagel and Schreckenberg, in 1992. This model was successfully improved and is still employed by several researchers (Chen and Wang, 2016; Hua, Yue, Wei, Chen, and Wang, 2020; Lan and Chang, 2005; Lan, Chiou, Lin, and Hsu, 2010; Lv, Song, Liu, and Ma, 2013; (Sean) Qian, Li, Li, Zhang, and Wang, 2017; Ruan, Zhou, Tu, Jin, and Shi, 2017; Yang, Qiu, Yu, Sun, and Pu, 2015; Zeng et al., 2021).

The modeled track has 2 000 cells with a length of 3,75 m each, totaling 7,5 km. Cars have 11 speeds from 0 to 135 km/h, and motorcycles have 5, from 0 to 54 km/h. Cars can travel on the left side of the lane and motorcycles can travel on both sides; therefore, motorcycles can split the lane with cars and other motorcycles. Additionally, this model attempts to represent the motorcycle's notable ability to weave through traffic at lower speeds (Figure 1).

The traffic simulation has five steps, similar to the one proposed by Meng et al. (2007). Those steps are proposed both to manage the lateral and longitudinal movement and to provide safety for the vehicles, avoiding collisions. Table 2 lists the parameters and variables employed during the procedure.

Table 2. Summary of variables and parameters employed in the traffic model

Variable	Description
$v_{\max}^{(m)}$	Maximum velocity of the motorcycle
$v_{\max}^{(c)}$	Maximum velocity of the car
p	Deceleration probability
d	Number of spaces the vehicle look ahead
$x_n^{(m)}$	Position of the nth motorcycle
$x_n^{(c)}$	Position of the nth car
$v_n^{(m)}$	Velocity of the nth motorcycle
$v_n^{(c)}$	Velocity of the nth car
g_+	Gap on the target lane in front of the motorcycle
g_-	Gap on the target lane behind the motorcycle
$d_n^{(c)}$	Gap between the nth car and the vehicle ahead
$d_n^{(m)}$	Gap between the nth motorcycle and the vehicle ahead
$g_-^{(mc)}$	Gap between the nth motorcycle and the nearest car behind it
v_{ll}	Velocity of the vehicle on the left lane considering d
v_{rl}	Velocity of the vehicle on the right lane considering d

Source: Based on Meng et al. (2007)

To summarize, motorcycles decide if it is worth changing sides depending on traffic conditions. In the second and third steps, all vehicles accelerate or decelerate respecting the non-collision rule and their maximum speed. In the fourth step, a braking probability is introduced for all vehicles (p = 0,10), in an attempt to represent driver's distraction in real traffic. Without this step, all vehicles would move together with the same speed, as train wagons. We consider that the vehicles leaving the track return to the beginning to maintain constant densities (periodical boundary condition). In the final step, all vehicles move as previously evaluated.

Step 1: Verify the lane-changing procedure (*if positive, the motorcycle changes lane*)

a. From the right to the left lane:

   if $v_n^{(m)} \le g_+$ and $g_- \ge v_{\max}^{(c)}$ and $v_{rl} \le v_{ll}$ and $v_{rl} \le v_n^{(m)}$

b. From the left to the right lane: if $\left(v_n^{(m)} \le g_+\right.$ and $\left.g_- \ge v_{\max}^{(m)}\right)$ and $\left(g_-^{mc} = 0 \text{ or } v_{rl} \ge v_n^{(m)} \text{ or } v_{rl} \ge v_{ll}\right)$

Step 2: Acceleration of the vehicles

a. Cars: $v_n^{(c)} \rightarrow \min\left(v_n^{(c)}+1, v_{\max}^{(c)}\right)$

b. Motorcycles: $v_n^{(m)} \rightarrow \min\left(v_n^{(m)}+1, v_{\max}^{(m)}\right)$

Step 3: Deceleration of the vehicles

a. Cars: $v_n^{(c)} \rightarrow \min(v_n^{(c)}, d_n^{(c)})$

b. Motorcycles: $v_n^{(m)} \rightarrow \min(v_n^{(m)}, d_n^{(m)})$

Step 4: Randomization (with the probability p)

a. Cars: $v_n^{(c)} \rightarrow \max(v_n^{(c)} - 1, 0)$

b. Motorcycles: $v_n^{(m)} \rightarrow \min(v_n^{(m)} - 1, 0)$

Step 5: Movement of the vehicles

a. Cars: $x_n^{(c)} \rightarrow x_n^{(c)} + v_n^{(c)}$

b. Motorcycles: $x_n^{(m)} \rightarrow x_n^{(m)} + v_n^{(m)}$

The traffic model receives the inputs from the engine and vehicle models and calculates two important factors in every time step: the speed of every vehicle i, $v_{i,t}^{(m,c)}$ (m = motorcycle, or c = car), and the energy consumed by each vehicle, $e_{i,t}^{(m,c)}$. The densities of the vehicles: motorcycles ($\rho^{(m)}$, [motorcycle/m]) and cars ($\rho^{(c)}$,[car/m]), are calculated through Equation (5):

$$\rho^{(m,c)} = \overline{\overline{\left(\frac{n^{(m,c)}}{L_{\text{sim}}}\right)}} \tag{5}$$

where $n^{(m,c)}$ is the number of motorcycles ($n^{(m)}$) or cars ($n^{(c)}$), and L_{sim} is the length of the simulated track (7 500 m). A double average is applied to decrease the influence of the initial condition, one on time and other between simulations. Similarly, the average speed of the vehicles, $V^{(m,c)}$ [m/s], Equation (6), is given by the double average among all the vehicles on the track in the last 1 000 seconds of 30 simulations.

$$V^{(m,c)} = \overline{\overline{\left(\frac{\sum v_{i,t}^{(m,c)}}{n^{(m,c)}}\right)}} \tag{6}$$

The flow of occupants for each type of vehicle, $Q^{(m)}$ [motorcycle occupant/s] and $Q^{(c)}$ [car occupant/s] is given by Equation (7), as the product of the occupancy rate $o^{(m,c)}$ [occupant/vehicle], the vehicle density $\rho^{(m,c)}$, and the average speed $V^{(m,c)}$. In this study, the occupancy rate for cars and motorcycles is considered equal to 1.

$$Q^{(m,c)} = o^{(m,c)} \rho^{(m,c)} V^{(m,c)} \tag{7}$$

The total flow of occupants on the track Θ (occupant/s), Equation (8), is the sum of the flow of motorcycle and car occupants.

$$\Theta = Q^{(m)} + Q^{(c)} \tag{8}$$

In this study, new metrics are introduced in relation to (Meng et al., 2007), which is possible with the use of the engine and vehicle models. The average consumed energy by vehicle by distance, $E^{(m,c)}$ [J/vehicle·m] is given by Equation (9).

$$E^{(m,c)} = \frac{1}{V^{(m,c)}} \overline{\overline{\left(\frac{\sum e_{i,t}^{(m,c)}}{n^{(m,c)} \Delta t}\right)}} \tag{9}$$

The total consumed energy, by time and space, Ξ (J/m·s) is given by the sum of the consumption of motorcycles and cars, as provided by Equation (10). From the energy consumption, it is possible to estimate the CO_2 emissions since they are proportional. We consider the combustion of each MJ of C_8H_{18} to emit 0,07 kg of CO_2.

$$\Xi = E^{(m)} V^{(m)} \rho^{(m)} + E^{(c)} V^{(c)} \rho^{(c)} \tag{10}$$

Table 3. Financial considerations

Parameter	Car	Motorcycle
Engine displacement	1 000 cm^3	125 cm^3
L_m, monthly distance [km]	315 km	
λ, monthly interest rate	0,01	
κ, number of months	48	
S_m, monthly wage [US$]	580	
H_m, monthly hours of work [h]	168	
V_p, vehicle acquisition [US$]	8 200	1 600
V_s, vehicle reselling [US$]	5 700	1 200

Source: Authors

Table 3 lists the Brazilian financial parameters employed in the calculation of monthly costs, $C^{(m,c)}$ (US$/occupant·month), Equation (11). In this Equation, the first term on the right-hand side represents the monthly value relative to the vehicle acquisition, V_p. To compare monthly equivalent values, the corrected number of months μ is employed, which is calculated by Equation (12) (Stoecker, 1989) and considers the monthly interest rate λ and the number of financed months κ used in the analysis. The second term of Equation (11) represents the monthly equivalent of the reselling value of the vehicle, V_s. The third term calculates the operational cost with fuel, considering a fuel tariff σ (US$/J), the monthly traveled distance L_m, and a factor ε to consider taxes, maintenance, and parking. The last term considers time lost in traffic, while taking the monthly wage S_m into account, which the occupant earns for working H_m hours.

$$C^{(m,c)} = \frac{V_p}{o^{(m,c)}\mu} - \frac{V_s}{o^{(m,c)}\mu(1+\lambda)^{\kappa}} + \frac{(1+\varepsilon)\,\sigma E^{(m,c)}}{o^{(m,c)}}\frac{L_m}{V^{(m,c)}} + \frac{S_m}{H_m}\frac{L_m}{V^{(m,c)}} \tag{11}$$

$$\mu = \frac{(1+\lambda)^{\kappa} - 1}{\kappa(1+\lambda)^{\kappa}} \tag{12}$$

The complete simulation can be summarized in three steps. First, the vehicle model (Equation 3) is linked to the engine model (Equations 1 and 2) to calculate energy consumption (Equation 4) for all possible situations of traffic (constant speed, acceleration, and braking). In the second step, the traffic simulations are performed (five steps procedure), where 189 traffic conditions were studied, with 27 car densities (0 to 130 cars/km, as well as motorcycle densities (0 to 213,3 motorcycles/km). In the last step, the traffic and the energy vectors are united (Figure 2) to calculate vehicle flow (Equation 7), energy consumption (Equation 9) and financial costs (Equation 11) for each traffic condition. Other relevant parameters managed during the simulation process include vehicle gear (j), which is related to the engine speed (ω) based on the simulated vehicle gear ratio, and lane (l). In this study, all equations are described in SI units. However, in figures and tables, numbers are displayed in more usual units.

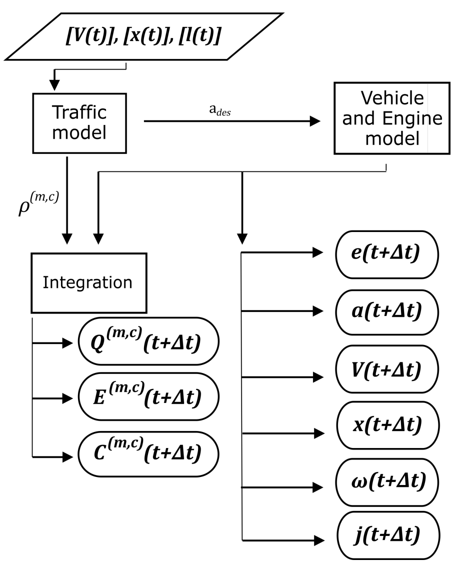

Figure 2. Summary of the Integration between the models.
Source: Authors

Results and discussion

The fundamental diagram of cars (Figure 3) presents the results of our computational algorithm reproducing Meng et al. (2007). Examining the curve for $\rho^{(m)} = 0$ (no motorcycles), as car density $\rho^{(c)}$ increases, car flow (Equation 7) increases up to $\rho^{(c)} = 20$. Car flow decreases from critical density until jam density is $\rho^{(c)} = 130$. This occurs because, under low-density conditions, cars are free to move at the maximum desired speed. However, as the number of cars increases, their movement is disturbed, thus reducing flow. The maximum car flow is 2 404 cars per hour, and it happens in absence of motorcycles ($\rho^{(m)} = 0$), as well as at a low car density ($\rho^{(c)} = 20$). In addition, examining motorcycle influence on car flow, as the density $\rho^{(m)}$ increases, car flow decreases. This happens because motorcycles can travel on both lanes of the road, which disturbs car flow.

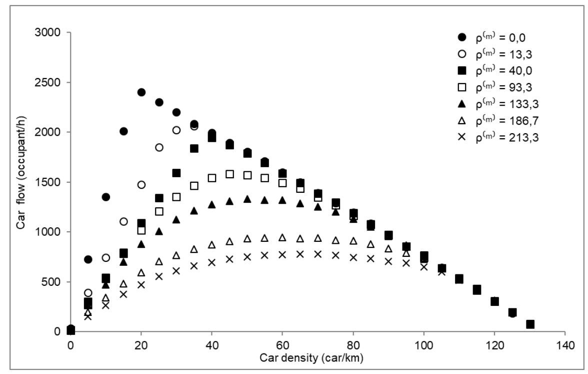

Figure 3. Fundamental diagram for cars.
Source: Authors

Figure 4 displays the total vehicle flow (Equation 8) as a function of the total density. When traffic is seen from this point of view, a higher density of motorcycles increases the total flow of vehicles up to 93,3 motorcycles/km. Figure 3 indicates that motorcycles can increase the passenger flow as high as 78% per lane, from 2 404 (cars only) to 4 291 vehicles per hour (cars and motorcycles).

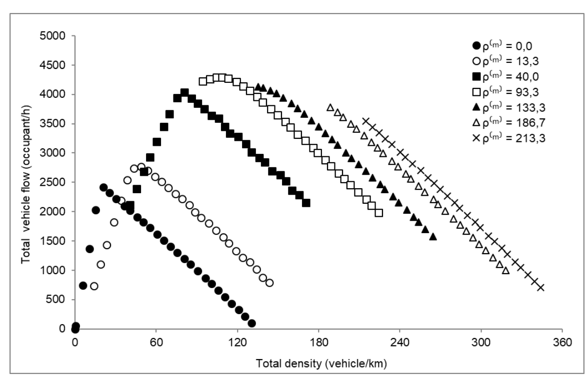

Figure 4. Fundamental diagram for vehicles (cars and motorcycles).
Source: Authors

It is possible to calculate the average speed from Figures 3 and 4 using Equation (7). From the fundamental diagram, it can be seen that the speed for cars is maximum until critical density is reached; and decreases to zero at maximum density, following the pattern described by Daganzo (1994). For motorcycles, when density is low, their average speed is constant for all car densities. As expected, their average speed decreases when motorcycle and car density increases further.

In the next phase of the study, energy consumption Equation (9) is analyzed. Having performed a scale analysis on

Equation (3), it can be concluded that energy consumption is predominantly a function of inertia (re-acceleration) and aerodynamic drag (speed). The force of gravity can also be crucial, but, in this study, we have a null inclination. The behavior of energy consumption for cars per km (Figure 5) is explained by two phenomena: as the density increases, the average speed decreases, hence diminishing drag resistance and increasing the time spent for the same displacement. It also increases the frequency of accelerations.

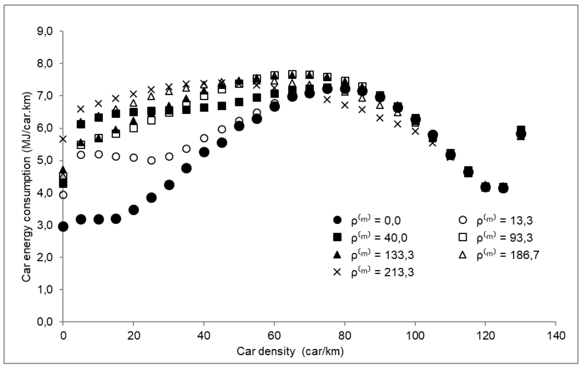

Figure 5. Car energy consumption.
Source: Authors

The increased energy consumption for cars until car density reaches $\rho^{(c)} = 80$ is caused by the increase in the frequency of re-accelerations (drag is almost constant). When $\rho^{(c)} > 80$, the decrease of car energy consumption occurs both because of the decreasing average speed and decreasing re-acceleration frequency. For very high car densities ($\rho^{(c)} > 130$), another increase in consumption is noticed, which is caused by the large amount of time spent in the traffic jam. In Figure 5, it is seen that modifying the motorcycle density for the same car density affects the average car fuel consumption, that is, increasing the motorcycle density also increases the car energy consumption.

Figure 6 presents the results of energy consumption for motorcycles. For lower motorcycle densities ($\rho^{(m)} = 13{,}3$ and $\rho^{(m)} = 40{,}0$), consumption is not affected by cars or other motorcycles in the track. For medium and higher motorcycle densities, consumption qualitatively follows the reacceleration frequency.

While examining the total energy consumption (Figures 7 and 8), some trends can be noticed. First, for the same total flow, it is better to have a higher proportion of motorcycles, since motorcycles are more fuel-economic than cars. Second, in the region of higher total flow ($\rho^{(m)} = 93{,}3$, $0 < \rho^{(c)} < 50$), increasing car density can triplicate the energy consumption (consequently, CO_2 emission) with insignificant benefit to the total vehicle flow. Another effect that is worth to discuss, it that for $\rho^{(m)} < 93{,}3$ (Figure 7), an increase in car density tends first to increase the total flow up to its maximum value. On the other hand, for densities $\rho^{(m)} > 93{,}3$ (Figure 8) an increase in the number of cars always decreases the total flow for the same motorcycle density.

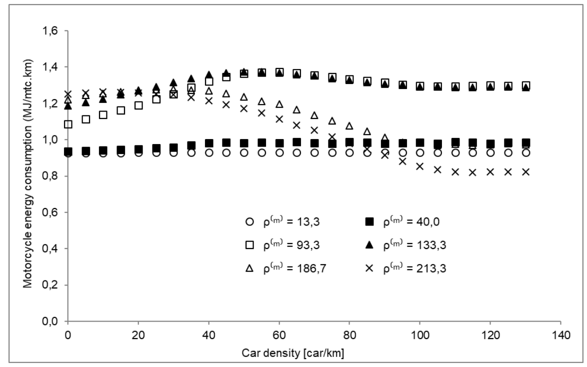

Figure 6. Motorcycle energy consumption.
Source: Authors

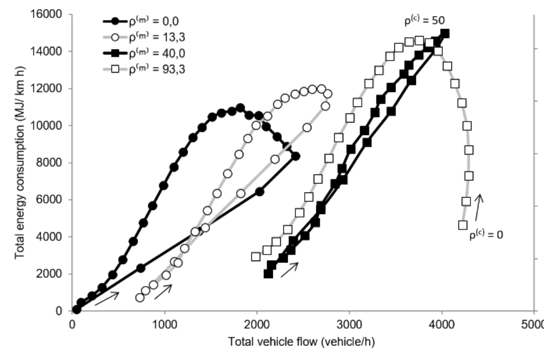

Figure 7. Total energy consumption ($0 \leq \rho^{(m)} \leq 93{,}3$).
Source: Authors

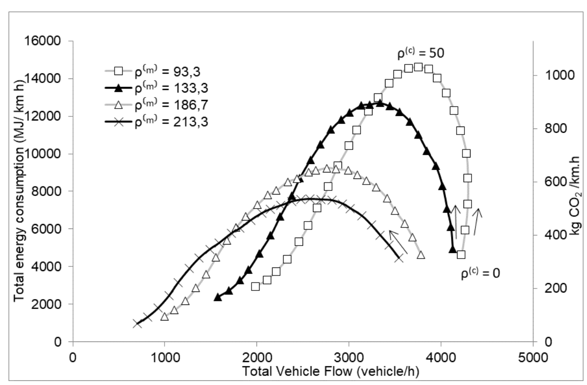

Figure 8. Total energy consumption ($93{,}3 \leq \rho^{(m)} \leq 213{,}3$).
Source: Authors

The last metric to be analyzed is individual cost, considering the purchase and reselling of the vehicle, fuel consumption, maintenance, taxes, parking, and the cost of the time spent in traffic (Equation 11) according to the financial considerations informed in Table 3. Figure 9 presents the individual costs for cars in function of the densities of cars and motorcycles. It is possible to notice that the higher the number of cars, the higher is the monthly cost. This happens because of two reasons. First, for the same motorcycle density, as car density increases, the average speed decreases, hence increasing the time spent in traffic. The second effect is fuel consumption (Figure 5). From zero to intermediate densities, consumption increases with car density. For higher densities, consumption decreases with car density, but it is not enough to compensate for the time lost. A higher motorcycle density increases car costs.

Figure 10 presents the individual costs for motorcycles. By comparing them with the monthly car cost (Figure 9), it is possible to notice that the costs for motorcycles are always lower, since they are cheaper and their fuel consumption is lower. Cars do not strongly influence motorcycle costs for low and medium motorcycle densities.

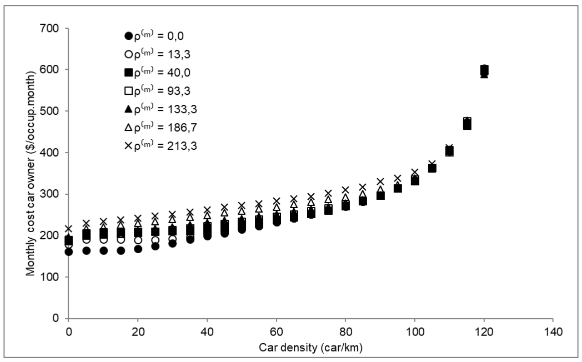

Figure 9. Monthly car cost.
Source: Authors

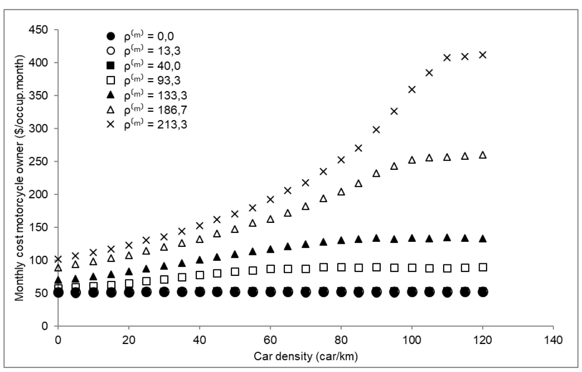

Figure 10. Monthly motorcycle cost.
Source: Authors

Conclusions

According to this analysis, the best scenario can be determined from each point of view. For car drivers, considering the objective of travelling at a higher average speed, the best scenario occurs in the absence of motorcycles ($\rho^{(m)} = 0$) and with a low car density ($\rho^{(c)} < 20$). Considering individual costs, car drivers would rather have an empty road, without other cars ($\rho^{(c)} = 0$) or motorcycles ($\rho^{(m)} = 0$). For motorcycle riders, from the point of view of average speed, a low motorcycle density ($\rho^{(m)} \leq 40$) would be compelling because they would travel through traffic at maximum speed. The same condition also is interesting financially, since for motorcycles the cost due to lost time is the more relevant.

For society, the metrics should be others. From the point of view of vehicle flow, it would be interesting to have few cars ($\rho^{(c)} = 15$) and an intermediate presence of motorcycles ($\rho^{(m)} = 93{,}3$), with a total density of $\rho = 108{,}3$, as seen in the fundamental diagram for vehicles (Figure 4). Considering CO_2 emissions as proportional to energy consumption (Figures 7 and 8) for a determined flow, a higher motorcycle proportion is responsible for lower the consumption on the track, since motorcycles are more fuel-economic. This study concludes that, for the same total flow, the relative density of cars and motorcycles can have a huge impact on the total CO_2 emissions of the road.

As hypothesized in the introduction, we conclude that the best traffic conditions depend on the metric (*e.g.*, average speed, flow, CO_2, and costs) and on the point of view (individual or social). It is shown that that the percentage of motorcycles and cars strongly influences the metrics. These results inform that it is not feasible to use results from one study (*e.g.*, richer countries with homogeneous traffic conditions and a small motorcycle fleet) to analyze another one (*e.g.*, developing countries with a mixed traffic of cars of cars and motorcycles), even though both may have the same total flow of vehicles.

Acknowledgements

The authors would like to thank the Coordenação de Aperfeiçoamento de Pessoal de Nível Superior (CAPES) for their scholarship support.

References

Agarwal, A., Zilske, M., Rao, K. R., and Nagel, K. (2015). An elegant and computationally efficient approach for heterogeneous traffic modelling using agent based simulation. *Procedia Computer Science, 52*(1), 962-967. 10.1016/j.procs.2015.05.173

Andrade, G. M. S. de, Araújo, F. W. C. de, Santos, M. P. M. de N., and Magnani, F. S. (2020). Standardized Comparison of 40 Local Driving Cycles: Energy and Kinematics. *Energies*, 13(20), 5434. 10.3390/en13205434

Arun, N. H., Mahesh, S., Ramadurai, G., and Shiva Nagendra, S. M. (2017). Development of driving cycles for passenger cars and motorcycles in Chennai, India. *Sustainable Cities and Society, 32*(March), 508-512. 10.1016/j.scs.2017.05.001

Ben-Chaim, M., Shmerling, E., and Kuperman, A. (2013). Analytic modeling of vehicle fuel consumption. *Energies, 6*(1), 117-127. 10.3390/en6010117

Chen, Q. and Wang, Y. (2016). A cellular automata (CA) model for motorized vehicle flows influenced by bicycles along the roadside. *Journal of Advanced Transportation*, *50*(6), 949-966. 10.1002/atr.1382

Cossalter, V. (2006). *Motorcycle Dynamics* (2nd Ed.). Morrisville, NC: LULU.com

Daganzo, C. F. (1994). The cell transmission model: a dynamic representation of highway traffic consistent with the hydrodynamic theory. *Transportation Research Part B: Methodological*, *28*(4), 269-287. 10.1016/0191-2615(94)90002-7

Ehsani, M., Ahmadi, A., and Fadai, D. (2016). Modeling of vehicle fuel consumption and carbon dioxide emission in road transport. *Renewable and Sustainable Energy Reviews, 53*, 1638-1648. 10.1016/j.rser.2015.08.062

Gössling, S. and Choi, A. S. (2015). Transport transitions in Copenhagen: Comparing the cost of cars and bicycles. *Ecological Economics, 113,* 106-113. /10.1016/j.ecolecon.2015.03.006

Hua, W., Yue, Y., Wei, Z., Chen, J., and Wang, W. (2020). A cellular automata traffic flow model with spatial variation in the cell width. *Physica A: Statistical Mechanics and Its Applications*, *556*, 124777. 10.1016/j.physa.2020.124777

Jazar, R. N. (2014). *Vehicle Dynamics* (2nd Ed.). New York, NY: Springer-Verlag. 10.1007/978-1-4614-8544-5

Koossalapeerom, T., Satiennam, T., Satiennam, W., Leelapatra, W., Seedam, A., and Rakpukdee, T. (2019). Comparative study of real-world driving cycles, energy consumption, and CO_2 emissions of electric and gasoline motorcycles driving in a congested urban corridor. *Sustainable Cities and Society, 45*(September 2018). 10.1016/j.scs.2018.12.031

Lan, L. W. and Chang, C.-W. (2005). Inhomogeneous cellular automata modeling for mixed traffic with cars and motorcycles. *Journal of Advanced Transportation*, *39*(3), 323-349. 10.1002/atr.5670390307

Lan, L. W., Chiou, Y. C., Lin, Z. S., and Hsu, C. C. (2010). Cellular automaton simulations for mixed traffic with erratic motorcycles' behaviours. *Physica A: Statistical Mechanics and Its Applications*, *389*(10), 2077-2089. 10.1016/j.physa.2010.01.028

Lv, W., Song, W. G., Liu, X. D., and Ma, J. (2013). A microscopic lane changing process model for multilane traffic. *Physica A: Statistical Mechanics and Its Applications*, *392*(5), 1142-1152. 10.1016/j.physa.2012.11.012

Meng, J., Dai, S., Dong, L., and Zhang, J. (2007). Cellular automaton model for mixed traffic flow with motorcycles. *Physica A: Statistical Mechanics and Its Applications, 380*, 470-480. 10.1016/j.physa.2007.02.091

Nagel, K. and Schreckenberg, M. (1992). A cellular automaton model for freeway traffic. *Journal de Physique, 2*, 2221-2229. 10.1051/jp1:1992277

Ni, D. and Henclewood, D. (2008). Simple engine models for VII-enabled in-vehicle applications. *IEEE Transactions on Vehicular Technology, 57*(5), 2695-2702.10.1109/TVT.2008.917229

Qian, Z., Li, J., Li, X., Zhang, M., and Wang, H. (2017). Modeling heterogeneous traffic flow: A pragmatic approach. *Transportation Research Part B: Methodologica*l, 99, 183-204. 10.1016/j.trb.2017.01.011

Ruan, X., Zhou, J., Tu, H., Jin, Z., and Shi, X. (2017). An improved cellular automaton with axis information for microscopic traffic simulation. *Transportation Research Part C: Emerging Technologies*, *78*, 63-77. 10.1016/j.trc.2017.02.023

Stoecker, W. F. (1989). *Design of Thermal Systems* (3rd Ed.). New York, NY: McGraw-Hill.

Tranter, P. (2012). Effective Speed: Cycling Because It's "Faster." In J. Pucher and R. Buehler (Eds.) *City Cycling* (*Urban and Industrial Environments*). Boston, MA: MIT Press.

WHO (World Health Organization). (2015). *Global status report on road safety*. http://apps.who.int/iris/bitstream/10665/189242/1/9789241565066_eng.pdf

Yang, D., Qiu, X., Yu, D., Sun, R., and Pu, Y. (2015). A cellular automata model for car-truck heterogeneous traffic flow considering the car-truck following combination effect. *Physica A: Statistical Mechanics and Its Applications, 424*, 62-72. 10.1016/j.physa.2014.12.020

Zegeye, S. K., De Schutter, B., Hellendoorn, J., Breunesse, E. A., and Hegyi, A. (2013). Integrated macroscopic traffic flow, emission, and fuel consumption model for control purposes. *Transportation Research Part C: Emerging Technologies, 31*, 158-171. 10.1016/j.trc.2013.01.002

Zeng, J., Qian, Y., Mi, P., Zhang, C., Yin, F., Zhu, L., and Xu, D. (2021). Freeway traffic flow cellular automata model based on mean velocity feedback. *Physica A: Statistical Mechanics and its Applications*, 562, 125387. 10.1016/j.physa.2020.125387